In Situ Laser Activation of Glassy Carbon Electrodes

Melanie Poon and Richard L. McCreery*

Department of Chemistry, The Ohio State University, Columbus, Ohio 43210

Laser pulses of short duration (10 ns) and high intensity (20 MW cm^{-2}) can increase the rate of heterogeneous electron transfer at a glassy carbon electrode by 1–3 orders of magnitude. The laser pulse may be delivered in situ, directly in the solution of interest, repeatedly if desired. The heterogeneous electron transfer rate constant, $k°$, for the ferri-/ferrocyanide redox system increases from 0.004 to 0.20 cm s^{-1} with laser activation, resulting in the highest $k°$ yet observed for this system on glassy carbon. Laser activation results in minor morphological changes to the surface, as observed by scanning electron microscopy, mainly removal of an apparent layer of carbon microparticles. The technique holds promise as a means to repeatedly activate glassy carbon electrodes in situ, thus circumventing the need for renewal or reactivation by polishing or other ex situ treatments.

The wide use of the dropping mercury electrode (DME) stems from its renewable surface, a reproducible electrochemical response for each drop, and measurements that are devoid of any electrode history effects. Solid electrodes have been studied extensively because they provide a wider potential range than mercury, have better mechanical properties, and can act in a catalytic role for reactions of importance to energy conversion, electrosynthesis, and electroanalysis. However, it has long been recognized that solid electrode behavior, unlike that of the DME, is highly dependent on history and that performance may be drastically altered by pretreatment procedures or processes occurring in the solution of interest (*1–7*). These alterations take the form of changes in heterogeneous electron transfer rate, increases in capacitance or surface Faradaic reactions, or in severe cases, total deactivation of the electrode. They often result in unstable and irreproducible analytical performance or complete destruction of electrocatalytic behavior.

Glassy carbon (GC) has been studied extensively in recent years because of its wide potential range, chemical inertness, relatively low cost, and low porosity. Mechanical polishing (*8–13*) and chemical (*14, 15*), electrochemical (*16–26*), thermal (*27, 28*), and rf plasma (*29, 30*) pretreatments have been used on carbon electrodes preceding an electrochemical experiment. The treatments were used to produce a surface as free as possible from contamination and to activate the electrode toward electron transfer. Hu, Karweik, and Kuwana (*13*) have compiled a variety of treatments for glassy carbon and noted that the heterogeneous electron transfer rate constant for the ferri-/ferrocyanide redox system can vary from 1.5×10^{-4} to 0.14 cm s^{-1} depending on pretreatment procedure. These workers reported the highest rate constant yet observed for this system on GC, 0.14 cm s^{-1}, and noted that this value is comparable to that for a platinum electrode.

While they can have large beneficial effects on electrode performance, none of the pretreatment procedures mentioned so far can be carried out quickly or repeatedly in the solution of interest, in a fashion analogous to the DME. In most cases, the electrode behavior degrades with time due to adsorption of impurities from the solution or chemical changes to the electrode surface, and the solid electrode becomes unsuitable for quantitative measurements. We recently reported a new, in situ method for cleaning and activating platinum and glassy carbon electrode surfaces using a short laser pulse delivered to the electrode directly in solution (*31*). The method is rapid and repeatable and was able to remove surface films and accelerate electron transfer by several orders of magnitude.

The present work was undertaken to provide a more quantitative and detailed understanding of in situ laser activation of glassy carbon electrodes. The overall goal of the work is a rapid in situ technique for producing GC surfaces with reproducibly high electron transfer rates.

EXPERIMENTAL SECTION

Electrochemical measurements were performed with a Bioanalytical Systems CV-1B potentiostat, a BAS Ag/AgCl (3 M NaCl) reference electrode, and Pt wire auxiliary electrode. For cyclic voltammetry above 0.2 V s^{-1}, a custom potentiostat driven by a function generator was used, with data recorded by a Tektronix 7854 digital oscilloscope. Heterogeneous electron transfer rate constants were determined from the anodic/cathodic peak separation using the method of Nicholson (*32*) with $\alpha = 0.5$. Apparent electrode capacitance was measured by the method introduced by Fagan, Hu, and Kuwana (*28*), where chronocoulograms are measured for each of a series of potential steps ranging in height from 50 to 150 mV. A plot of charge vs. potential step size yields the apparent capacitance.

The electrochemical cells shown in Figure 1 was constructed of Teflon, with a Pyrex window to allow laser light to impinge on the electrode after passage through the solution. The reference and auxiliary electrodes were placed without special attention to geometry, except at scan rates above 0.2 V s^{-1}, where a Luggin capillary was used between the reference and working electrodes. Unless noted otherwise, the working electrode consisted of a Tokai GC-20 or GC-20s disk pressed against a Teflon washer, which was exposed to the solution. The electrode area was defined by the hole in the washer, and equaled 0.012 cm^2 as measured by chronoamperometry. The entire exposed area was illuminated by the laser. In several experiments, a commercial (Bioanalytical Systems) GC electrode consisting of GC-30s carbon press fitted in Kel-F was employed. Most of the results reported here were obtained with the Tokai disk electrode design, but only minor differences were observed with the commercial electrode after activation.

Two different polishing procedures were employed. The procedure referred to as "conventional" consisted of polishing with 600-grit SiC paper followed by 1.0-, 0.3-, and 0.05-μm alumina in a slurry with Nanopure water on a Texmet (Buehler) polishing cloth. A more rigorous procedure was that of Hu, Karweik, and Kuwana (*13*), involving alumina on a glass plate with no cloth. In both procedures, the final electrode was thoroughly rinsed and sonicated. As noted below, the polishing procedure had no observable effect on the electrode performance after laser activation.

The laser was a Quantel 580-10 Nd:YAG laser capable of producing a 10-ns, 300-mJ pulse at 1064 nm. Experience with a different laser (Quanta-Ray DCR-2) indicated that beam quality is very important for this experiment, and erratic results were obtained if significant power density variations occurred across the electrode area. The laser beam was 6 mm in diameter, but only the center 1 mm reached the electrode. The power density across the 1-mm irradiated electrode area varied by approximately ±20%, as measured by a linear photodiode array after attenuation. A conventional thermal power meter (Scientech Model 38-0101) was used to measure the laser power passing through the Teflon

0003-2700/86/0358-2745$01.50/0

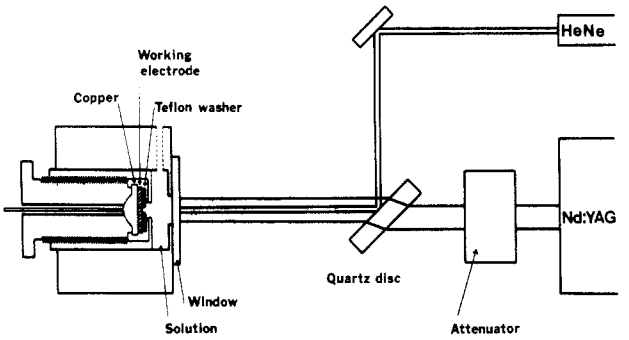

Figure 1. Experimental apparatus and optical arrangement. The He–Ne and Nd:YAG laser beams were colinear, and the Nd:YAG power was adjusted with the variable attenuator. The working electrode was defined by the Teflon washer pressed against the working electrode disk. Reference and auxiliary electrodes are not shown; the cell body was made of Teflon.

washer, which defined the working electrode. The power density was calculated by assuming the laser output was a square pulse of 10 ns duration. Power densities quoted here have an absolute accuracy of about ±20%, with some variation being unavoidable due to beam shape changes with laser tuning and alignment from experiment to experiment. The laser wavelength was 1064 nm for all experiments, and the power level was adjusted with a Newport Research Co. 935-5 beam attenuator. The optics were arranged as shown in Figure 1, such that the Nd:YAG beam was collinear with a low-power He–Ne beam, which was used to aim the activating pulse onto the electrode.

Despite reports on electrode filming with the ferri-/ferrocyanide redox system (*33*), it was used as a test system for comparing electron transfer rate constants because of the large volume of data available in the literature. Ascorbic acid, phenol, potassium ferrocyanide, *o*-chlorophenol, catechol, hydroquinone, Na_2SO_4, H_2SO_4, $HClO_4$, and KCl were reagent grade and used as received. Dopamine hydrochloride, NADH (98% grade III), 3,4-dihydroxyphenylacetic acid (DOPAC), and 3,4-dihydroxybenzylamine (DHBA) were obtained from Sigma Chemical Co. (St. Louis, MO). Unless noted otherwise, all solutions were prepared fresh daily using either NANOpure II water (Sybron Barnstead, Boston, MA) or water that had been triply distilled from dilute alkaline permanganate. Nitrogen purified by a Pall activated carbon filter (Pall Trinity Micro Corp., Cortland, NY) and an oxygen trap was used to degas solutions.

A Tencor Alpha Step profilometer based on vertical deflection of a 5-μm-diameter needle pulled across the surface was used to measure surface roughness. The vertical resolution was 100 Å, but the tip size resulted in integration of the measurement over a 5-μm region. Scanning electron microscopy was carried out with a ISI SX-30 microscope operated at 5 kV with a practical resolution of 100 Å.

RESULTS

The effect of laser activation on the cyclic voltammogram of the ferri-/ferrocyanide, $Fe(CN)_6^{3-/4-}$, redox couple is shown in Figure 2. After the dashed curve was taken, three 10-ns, 22 MW cm^{-2} laser pulses were delivered in rapid succession to the GC electrode; then the solid curve was obtained about 30 s after the last laser pulse. There is an obvious improvement in heterogeneous rate constant, resulting in a significant decrease in ΔE_p. Measurement of the heterogeneous electron transfer rate constant, $k°$, before and after activation indicated an increase from 0.004 ± 0.002 (N = 7) to 0.15 ± 0.01 (N = 7) cm s^{-1}, or a factor of 37. Quantitative effects of laser activation on $k°$ for $Fe(CN)_6^{3-/4-}$ are shown in Figure 3 as a function of laser power density. Little or no change in $k°$ is observed at powers below 9 MW cm^{-2}. Over the range from 12 to 24 MW cm^{-2}, $k°$ increases from 0.002 to a plateau at 0.20 ± 0.05 cm s^{-1}, which remains flat at least up to 60 MW cm^{-2}. As shown in Figure 4, $k°$ decreases slowly with time after the laser pulse when the electrode is allowed to stand in Nanopure electrolyte, with a faster decay rate observed in less pure

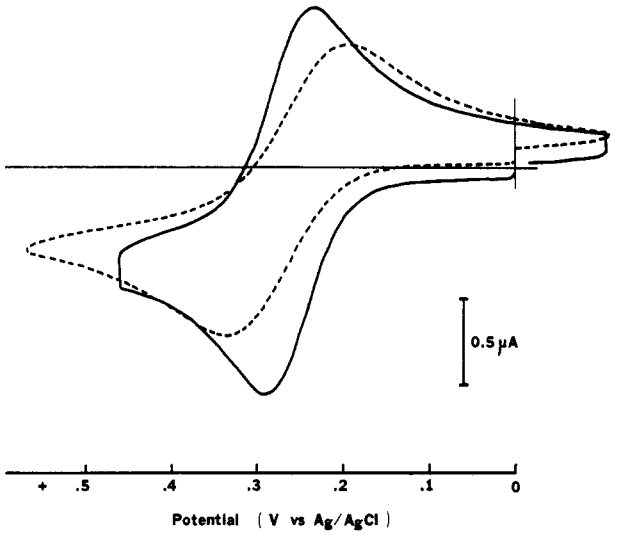

Figure 2. Effect of three 22 MW cm^{-2}, 10-ns laser pulses on the voltammogram of 1.0 mM ferrocyanide in 1 M KCl, scan rate = 0.1 V s^{-1}. Dashed curve is after conventional polishing with a polishing cloth. Solid curve is after laser activation.

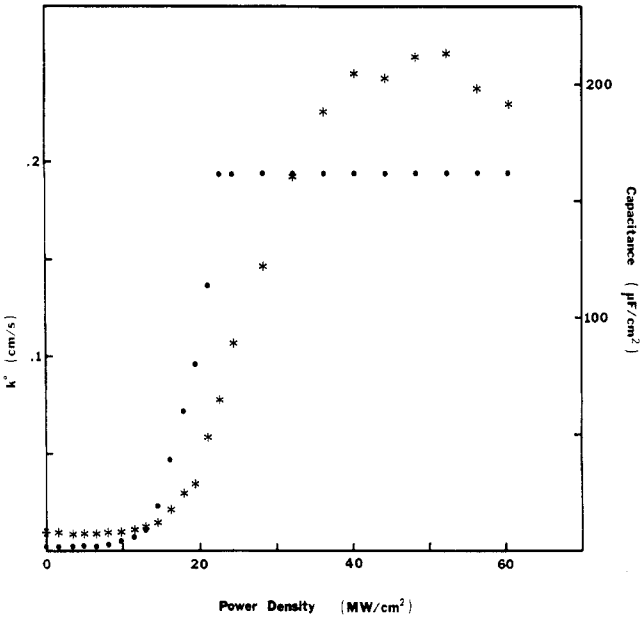

Figure 3. Observed $k°$ (points) for $Fe(CN)_6^{3-/4-}$ (1.0 mM in 1.0 M KCl) and capacitance (asterisks) as functions of laser power density.

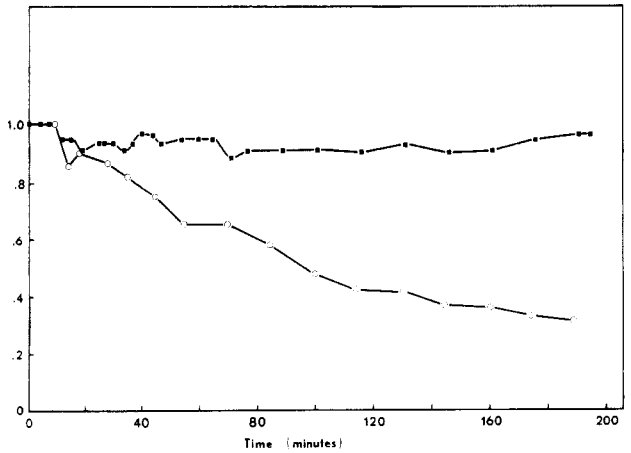

Figure 4. Time course of $k°$ for $Fe(CN)_6^{3-/4-}$ after laser activation. Values are normalized to their magnitudes immediately after the pulse; conditions are same as in Figure 3. Squares are $k°$ in Nanopure water; points are $k°$ in double-distilled water.

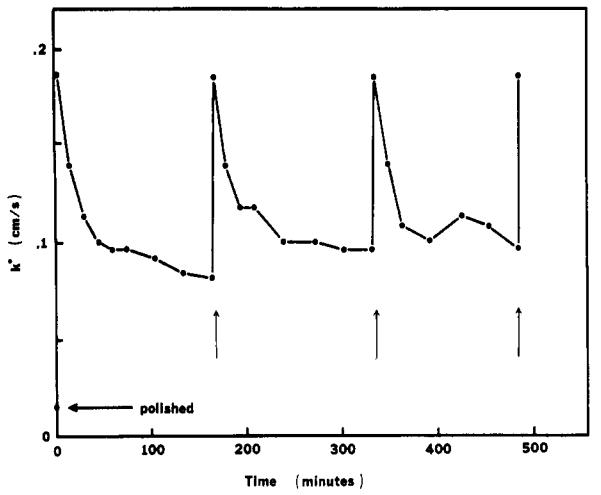

Figure 5. $k°$ vs. time for $Fe(CN)_6^{3-/4-}$ in 1.0 M KCl, in double-distilled water. Conventional polishing led to the first point, at 0.01 cm s^{-1}; then an increase to 0.19 cm s^{-1} occurred after three laser pulses at 22 MW cm^{-2}. Single laser pulses were applied at 180, 340, and 490 min.

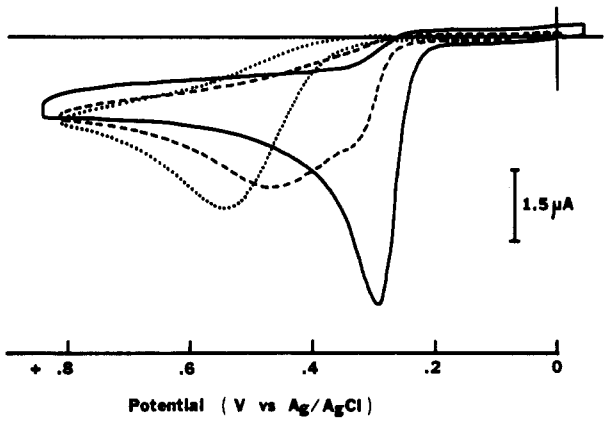

Figure 6. Effect of in situ laser irradiation on the voltammetry of 1.0 mM ascorbic acid in 0.1 M H_2SO_4. Dotted curve was obtained on conventionally polished GC, dashed curve after three 20 MW cm^{-2} pulses, solid curve after three 28 MW cm^{-2}.

double-distilled water. Figure 5 demonstrates that the activation process could be repeated by delivering single laser pulses in situ after deactivation with standing in double-distilled water.

The effect of laser pulses on the voltammetry of ascorbic acid on GC is shown in Figure 6. The conventional polishing procedure yields a voltammetric oxidation peak at 0.6 V vs. Ag/AgCl with considerable variation from run to run. Laser activation at 20 MW cm^{-2} results in partial activation, with a peak shift to 0.450 V. An increase in power density to 28 MW cm^{-2} results in full activation to a peak potential of 0.295 V, and further increases in power did not yield further peak potential shifts. The present results differ from those in our previous communication on laser activation (*31*) because the entire electrode is irradiated rather than small spots, yielding a fully activated surface and a voltammogram comparable to that obtained from careful polishing or vacuum heat treatment. As estimated previously (*31*), the 300-mV shift in the ascorbic acid peak potential corresponds to an increase in $k°$ of greater than a factor of 10^3. The effect of activation on the voltammetry of a mixture of dopamine and ascorbic acid is shown in Figure 7, with complete resolution of the overlapped peaks being observed after the laser pulse. After activation, both ascorbic acid and dopamine oxidize at nearly their thermodynamic potentials, whereas before activation, both systems exhibit slow electron transfer kinetics. The lifetime of activation for the ascorbic acid and dopamine systems is

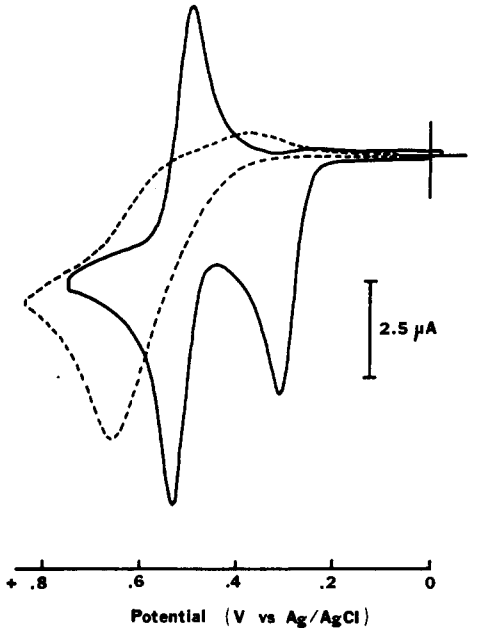

Figure 7. Effect of laser activation on the voltammetry of a mixture of 1.0 mM dopamine and 1.0 mM ascorbic acid in 0.1 M H_2SO_4. Dashed curve is after conventional polishing; solid line is after three 25 MW cm^{-2} laser pulses.

Table I. Effect of Laser Activation on the Voltammetry of Several Redox Systems[a]

	before[b]			after[c]		
system	$E_{p,a}$	$E_{p,c}$	ΔE_p	$E_{p,a}$	$E_{p,c}$	ΔE_p
ascorbic acid	0.250			0.000		
NADH	0.480			0.335		
dopamine	0.260	0.135	0.125	0.200	0.168	0.032
O_2 1st wave		−0.725			−0.450	
2nd wave		−1.625			−1.475	
DOPAC	0.255	0.095	0.160	0.177	0.150	0.027
DHBA	0.355	0.120	0.235	0.230	0.200	0.030
catechol	0.290	0.132	0.158	0.206	0.181	0.025
ferrocyanide	0.325	0.225	0.100	0.300	0.243	0.057
hydroquinone	0.230	0.000	0.230	0.113	0.065	0.048

[a] 1 mM in 1 M KCl, 0.1 M phosphate, pH 7.0, scan rate = 0.1 V s^{-1}. [b] Conventional polishing with polishing cloth. [c] After three 20 MW cm^{-2} laser pulses in situ.

comparable to that observed for the $k°$ of $Fe(CN)_6^{3-/4-}$ noted in Figure 4. It was possible to repeatedly activate an electrode toward acsorbic acid oxidation over a period of 3 days, without removal or polishing of the electrode. Table I presents the results of voltammetry on a variety of compounds before and after laser activation. In all cases, the voltammetry is improved with laser activation, and in some cases the improvement is dramatic.

Activation was observed for either the $Fe(CN)_6^{3-/4-}$ or ascorbic acid redox system if the laser pulse occurred in air before the solution was added. Activation also occurred if the laser pulse was applied in blank electrolyte, which was then replaced with the ascorbic acid solution. These observations eliminate the possibility of any photolytic reactions of solution species contributing to the observed results, although such processes would be unexpected with 1064-nm light. It also indicates that liquid water is not essential for the activation process. In some cases, the electrode lost some of its activity during solution transfer or other handling, so in all experiments reported here, the laser pulse occurred in situ directly in the solution of interest.

The effects of laser activation on the morphology and elemental composition of the GC surface were assessed with

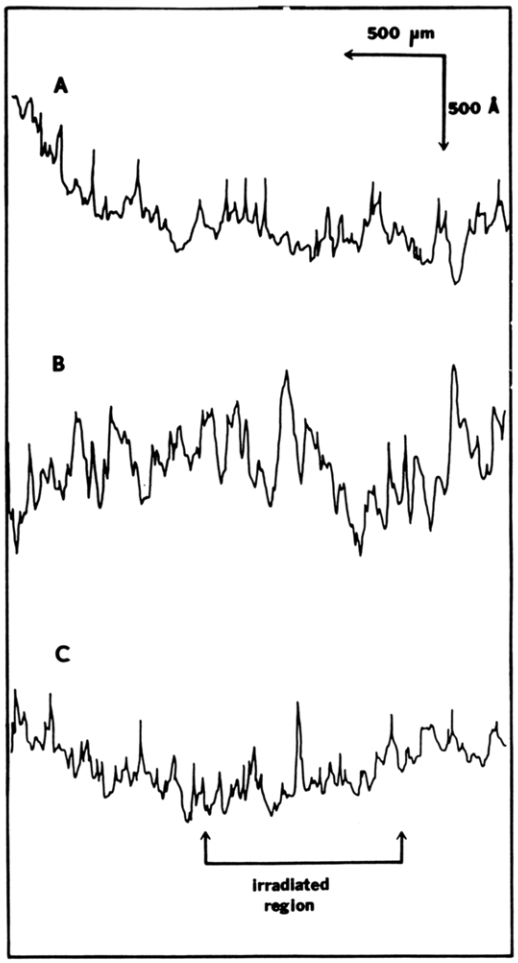

Figure 8. Profilometer traces of GC surfaces following polishing or laser activation. Upper trace was taken after polishing with 0.05-μm alumina, middle trace after 1.0-μm alumina. Lower trace was taken on an electrode polished with 0.05-μm alumina, then irradiated by three 40 MW cm^{-2} laser pulses in the indicated region.

optical and scanning electron microscopy (SEM), scanning Auger spectrometry (SAM), and a profilometer. Profilometer traces for an electrode polished with 1.0-μm alumina are reproducible and easily distinguished from those of an electrode polished with 0.05-μm alumina, as shown in Figure 8. There is no apparent difference between a nonirradiated, polished surface and an adjacent area that had received three 40 MW cm^{-2} laser pulses. These results indicate that a laser power density which is sufficient to activate the surface does not cause ablation or other gross changes in the GC surface on the scale of a few hundred angstroms. Scanning electron micrographs of polished and irradiated surfaces are shown in Figure 9. Micrograph A is an ordinary polished surface, showing the small pits common to glassy carbon, but no polishing scratches. The lack of apparent scratches has been attributed to a surface layer of carbon microparticles generated during polishing (*34*). After a 22 MW cm^{-2} laser pulse (Figure 9B), surface scratches appear, but no other changes are observable. At 40 MW cm^{-2}, surface scratches are more apparent and randomly oriented rings appear, presumably caused by diffraction from dust on the cell window.

SAM analysis of the GC surface was carried out after transferring the electrode through air from the cell to the SAM vacuum chamber. After laser irradiation (24 MW cm^{-2}) in 1 M KCl, the oxygen/carbon ratio was slightly lower for irradiated vs. nonirradiated regions of the same GC surface. For six electrodes the O/C ratio in the irradiated region was 62% (±17%) of its value in the nonirradiated region (average O/C ratio decreased from 0.07 to 0.04 upon irradiation). The

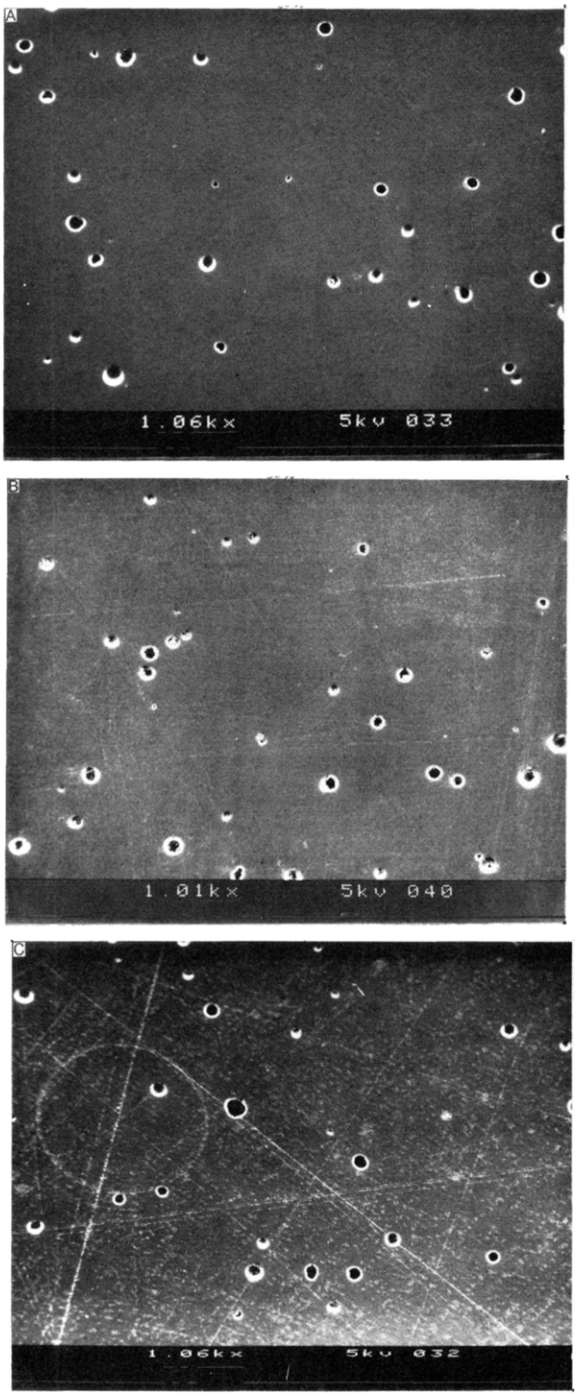

Figure 9. Scanning electron micrographs of polished and laser-activated GC surfaces: (A, top) conventionally polished surface, (B, middle) after activation with three 20 MW cm^{-2} laser pulses in solution, (C, bottom) after three 40 MW cm^{-2} pulses.

approximately 40% decrease in the O/C ratio implies removal of oxygen functional groups even when the irradiation occurs in water. No incorporation of potassium or chlorine was observed with the SAM at these power levels. Laser irradiation of a GC electrode in a high-vacuum environment yielded a decrease in the O/C ratio of 43% with a single pulse, as measured by ESCA. Further pulses and exposure to the ultra-high-vacuum environment lowered the surface oxygen to an immeasurably low level, implying that the laser is able to remove layers from the GC surface.

Laser activation at 20 MW cm^{-2} caused the voltammetric background current to increase by approximately a factor of 2. No new couples were observed with cyclic voltammetry, such as those attributed to surface quinone species (*11*, *12*,

35–37). The apparent capacitance measured by chronocoulometry is shown in Figure 3. A plot of capacitive charge vs. potential step amplitude was linear from −50 to 100 mV, with a slope proportional to the apparent capacitance. For an electrode polished conventionally (with a polishing cloth), the slope of such a plot corresponds to 10 ± 2.7 μF cm^{-2}, and this value increases to 23 ± 6.2 μF cm^{-2} after laser activation at 21 MW cm^{-2}. Using the same method for capacitance measurement, Kuwana and co-workers obtained 70 μF cm^{-2} for a freshly polished (no polishing cloth) activated electrode and a value of 10 μF cm^{-2} for a vacuum heat treated GC electrode (28). Note that irradiation with a power density of 21 MW cm^{-2} produces an increase of a factor of 37 in $k°$ for $Fe(CN)_6^{3-/4-}$, but only a factor of 2.3 in apparent capacitance.

DISCUSSION

The rate constant of 0.20 cm s^{-1} observed for $Fe(CN)_6^{3-/4-}$ on laser-activated GC is comparable to the best values obtained with other pretreatment procedures (0.12–0.14 cm s^{-1}) (13) and is in the range of the highest values observed for $Fe(CN)_6^{3-/4-}$ on a platinum electrode (0.20–0.24 cm s^{-1}) (5, 38). The plateau in the $k°$ vs. power density curve (Figure 3) implies that the surface condition no longer affects the rate constant and the observed rate is the upper limit for $Fe(CN)_6^{3-/4-}$ on either platinum or glassy carbon electrodes. The excellent performance of the laser-treated electrodes was obtained with a 10-ns pulse applied in situ, repeatedly if desired, and therefore circumvents the requirement for removal and often extensive polishing. Laser activation provides many of the features of the DME, particularly in situ renewability and reproducibility, but also retains the wide potential range of GC compared to mercury. In addition, solid electrode surfaces can exhibit electrocatalytic behavior provided they can be properly cleaned. The in situ laser activation technique circumvents the problem of slow electrode deactivation by adsorbed solution species.

The improvement in the voltammograms of ascorbic acid with laser activation is also comparable to that observed for other pretreatment procedures (27, 28), with the added feature of rapid in situ repeatability. The decrease in peak potentials for the oxidation of DOPAC, DHBA, ascorbic acid, and $Fe(CN)_6^{3-/4-}$ with 10-ns in situ laser pulses is comparable to or better than a heat treatment procedure involving several hours at reduced pressure (27). The ability to activate a variety of electron transfer reactions to exhibit near-Nernstian behavior may be of significant analytical value, particularly since a deactivated analytical sensor may be reactivated quickly without removal from the cell.

The extent of laser activation was largely independent of the polishing procedure. In many cases we purposely used a brief conventional polishing protocol employing a polishing cloth that is known to produce a low activity surface. Upon laser activation, this surface yielded $k°$ values comparable to the rigorous polishing procedure of Hu, Karweik, and Kuwana (13). Laser activation produced comparable $k°$ values, whether or not the rigorous polishing procedure was used, and was equally effective on commercial electrodes with Kel-F bodies. We chose to use a polishing cloth for most experiments presented here because the capacitance of the activated electrode was lower and the effects of laser activation were more obvious. Regardless of which preparation procedure we used, an active surface with $k°$ for $Fe(CN)_6^{3-/4-}$ >0.15 cm s^{-1} could be produced repeatedly in situ.

The profilometer and SEM results indicate that no gross change has occurred to the GC surface at laser powers sufficient to activate the surface. The only change observable at 20 MW cm^{-2} or below was the apparent removal of the surface microparticle film proposed by Kazee, Weisshaar, and Kuwana (34). It is clear that not only should powers above 20 MW cm^{-2} be avoided to minimize increases in capacitance and background current but also that 20 MW cm^{-2} is sufficient to activate the reactions studied here. The decrease in the surface O/C ratio revealed by Auger spectrometry implies that desorption or ablation of at least some surface layers occurs, but on a scale too small to be observed by SEM or the profilometer.

The increase in capacitance caused by laser activation could be caused by increases in microscopic surface area or by an increase in the capacitance per unit of microscopic area or both. The capacitance values observed here are intermediate between those for vacuum heat treatment (28) and highly polished surfaces (13), and the laser pulse can increase the capacitance by up to a factor of 24 at high power densities. Since there is no rigorous method to measure the microscopic surface area on carbon, it cannot be stated unequivocally that increases in capacitance imply proportional increases in microscopic area. However, it can be concluded rigorously that the electron transfer rate enhancements resulting from laser activation are not caused solely by increases in microscopic surface area. As noted earlier, an increase in capacitance by a factor of 2.3 is accompanied by an increase in $k°$ for $Fe(CN)_6^{3-/4-}$ by a factor of 37. Carefully polished surfaces (13) with more than 3 times higher capacitance (70 μF cm^{-2} vs. 23 μF cm^{-2}) have slightly lower rate constants than laser-activated GC. Furthermore, the apparent $k°$ for ascorbic acid increased by a much larger factor than the capacitance upon laser activation. The optimum power density range of 18–24 MW cm^{-2} was chosen as a compromise between capacitance and rate enhancement. At this power density, the $k°$ was not at its maximum, but the power density was not high enough to cause large increases in capacitance.

The areas of laser desorption mass spectrometry (39) and laser processing of materials have stimulated a large body of research on laser effects on surfaces (40, 41). However, there are few studies of laser effects carried out in solution, and those are limited to examinations of corrosion (42) and accelerated electroplating (43). Consequently, it is difficult to estimate the temperature achieved during a laser pulse or to predict what processes will occur on the surface.

Although other processes cannot yet be ruled out, it is possible to explain all of the observations made here, as well as many others that have been reported by a simple desorption mechanism. As proposed by others (13, 28), it is possible that the active sites on the GC surface are deactivated by the adsorption of trace materials encountered during preparation or during exposure to the solution of interest. In many preparation procedures, an active electrode is not produced because sufficient adsorbates are present in the polishing materials. If an active surface is achieved, whether by heat treatment, proper polishing, or laser activation, it is deactivated on a time scale of tens of minutes (or more quickly) by adsorption of pollutants from the solution. The laser activation process may be merely an effective means to remove such impurities, probably by a desorption process. Redox mediation and proton transfer have been proposed to explain accelerated electron transfer on carbon surfaces (13, 21, 30), and these mechanisms may be important for certain reactions. However, they do not appear to be involved in the accelerated oxidation of ascorbic acid or $Fe(CN)_6^{3-/4-}$ observed with laser activation or vacuum heat treatment. The changes in capacitance or possible changes in microscopic area with preparation procedure appear to be secondary to the desorption process, since they are not quantitatively correlated with electrode activity. Although the observed rate constant will depend upon the microscopic surface area, it is possible to observe high $k°$ values (≥0.14 cm s^{-1}) for $Fe(CN)_6^{3-/4-}$ on electrodes with a wide range of apparent capacitance (10–70

$\mu F\ cm^{-2}$) and presumably wide range of microscopic surface area.

ACKNOWLEDGMENT

We thank Daniel Fagan for carrying out the ESCA measurements. We also thank T. Kuwana, I.-F. Hu, R. Mark Wightman, and Royce Engstrom for useful discussions and for providing preprints of their papers on carbon activation.

Registry No. C, 7440-44-0; $Fe(CN)_6^{3-}$, 13408-62-3; $Fe(CN)_6^{4-}$, 13408-63-4; NaDH, 58-68-4; O_2, 7782-44-7; DOPAC, 102-32-9; DHBA, 37491-68-2; ascorbic acid, 50-81-7; catechol, 120-80-9; hydroquinone, 123-31-9; dopamine, 51-61-6.

LITERATURE CITED

(1) Adams, R. N. *Electrochemistry at Solid Electrodes*; Marcel Dekker: New York, 1969.
(2) Bishop, E.; Hitchcock, P. H. *Analyst (London)* **1973**, *98*, 475.
(3) Kinoshita, K. In *Modern Aspects of Electrochemistry*; Bockris, J. O'M., Conway, B. E., White, R. E., Eds.; Plenum: New York, 1982; p 557, and references therein.
(4) Amatore, C.; Saveant, J. M.; Tessier, D. *J. Electroanal. Chem.* **1983**, *146*, 37.
(5) Goldstein, E. L.; Van de Mark, M. R. *Electrochim. Acta* **1982**, *27*, 1079.
(6) S. Gilman *Lectroanal.* **1967**, *2*, 111.
(7) Conway, B. E.; et al. *Anal. Chem.* **1973**, *45*, 1331.
(8) Rusling, J. F. *Anal. Chem.* **1984**, *56*, 578.
(9) Kamau, G. N.; Willis, W. S.; Rusling, J. F. *Anal. Chem.* **1985**, *57*, 545.
(10) Thornton, D. C.; Corby, K. T.; Spendel, V. A.; Jordan, J.; Robbat, A.; Rutstrom, D. J.; Gross, M.; Ritzler, G. *Anal. Chem.* **1985**, *57*, 150.
(11) Laser, D.; Ariel, M. *J. Electroanal. Chem.* **1974**, *52*, 291.
(12) Gunsingham, H.; Fleet, B. *Analyst (London)* **1982**, *107*, 896.
(13) Hu, I. F.; Karweik, D. H.; Kuwana, T. *J. Electroanal. Chem.* **1985**, *188*, 59.
(14) Plock, C. E. *J. Electroanal. Chem.* **1969**, *22*, 185.
(15) Taylor, R. J.; Humffray, A. A. *J. Electroanal. Chem.* **1973**, *42*, 347.
(16) Engstrom, R. C. *Anal. Chem.* **1982**, *54*, 2310.
(17) Engstrom, R. C.; Strasser, V. A. *Anal. Chem.* **1984**, *56*, 136.
(18) Blaedel, W. J.; Jenkins, R. A. *Anal. Chem.* **1974**, *46*, 1952.
(19) Moiroux, J.; Elving, P. J. *Anal. Chem.* **1978**, *50*, 1056.
(20) Wightman, R. M.; Paik, E. C.; Borman, S.; Dayton, M. A. *Anal. Chem.* **1978**, *50*, 1410.
(21) Cabaniss, G. E.; Diamantis, A. A.; Murphy, W. R., Jr.; Linton, R. W.; Meyer, T. J. *J. Am. Chem. Soc.* **1985**, *107*, 1845.
(22) Wang, J.; Hutchins, L. D. *Anal. Chim. Acta* **1985**, *167*, 325.
(23) Wang, J. *Anal. Chem.* **1981**, *53*, 2280.
(24) Gonon, F. G.; Fombarlet, C. M.; Buda, M. J.; Pujol, J. F. *Anal. Chem.* **1981**, *53*, 1386.
(25) Rice, M. E.; Galus, Z.; Adams, R. N. *J. Electroanal. Chem.* **1983**, *143*, 89.
(26) Falat, L.; Cheng, H. Y. *J. Electroanal. Chem.* **1983**, *157*, 393.
(27) Stutts, K. J.; Kovach, P. M.; Kuhr, W. G.; Wightman, R. M. *Anal. Chem.* **1983**, *55*, 1632.
(28) Fagan, D. T.; Hu, I. F.; Kuwana, T. *Anal. Chem.* **1985**, *57*, 2759.
(29) Miller, C. W.; Karweik, D. H.; Kuwana, T. *Anal. Chem.* **1981**, *53*, 2319.
(30) Evans, J.; Kuwana, T. *Anal. Chem.* **1979**, *51*, 358.
(31) Hershenhart, E.; McCreery, R. L.; Knight, R. D. *Anal. Chem.* **1984**, *56*, 2257.
(32) Nicholson, R. S. *Anal. Chem.* **1965**, *37*, 1351.
(33) Kawaik, J.; Jedral, T.; Galus, Z. *J. Electroanal. Chem.* **1983**, *145*, 163.
(34) Kazee, B.; Weisshaar, D. E.; Kuwana, T. *Anal. Chem.* **1985**, *57*, 2736.
(35) Murray, R. W. *Electroanal. Chem.* **1984**, *13*.
(36) Panzer, R. E.; Elving, P. J. *Electrochim. Acta* **1975**, *20*, 635.
(37) Blurton, K. F. *Electrochim. Acta* **1973**, *18*, 869.
(38) Daum, P. H.; Enke, C. G. *Anal. Chem.* **1969**, *41*, 653.
(39) Harden, E. D.; Fan, T. P.; Blakley, C. R.; Vestal, M. L. *Anal. Chem.* **1984**, *56*, 2.
(40) Duley, W. W. *Laser Processing and Analysis of Materials*; Plenum: New York, 1983; p 89.
(41) Ready, J. F. *Effects of High Power Laser Radiation*; Academic Press: New York, 1971.
(42) Ulrich, R. K.; Alkire, R. C. *J. Electrochem. Soc.* **1981**, *128*, 1169.
(43) Kuiken, H. K.; Mikkers, F. E. P.; Wierenger, P. E. *J. Electrochem. Soc.* **1983**, *130*, 554.

RECEIVED for review March 26, 1986. Accepted July 1, 1986. This work was funded by the OSU Materials Research Laboratory and by the NSF Division of Chemical Analysis.

Amperometric Response of Microlithographically Fabricated Microelectrode Array Flow Sensors in a Thin-Layer Channel

Lawrence E. Fosdick and James L. Anderson*

Department of Chemistry, The University of Georgia, Athens, Georgia 30602

Thomas A. Baginski and Richard C. Jaeger

Alabama Microelectronics Science and Technology Center, Department of Electrical Engineering, Auburn University, Auburn University, Alabama 36849-3501

Microelectrode arrays were fabricated by use of photolithographic techniques. The electrodes consisted of gold metal deposited on a silicon substrate, pretreated by thermal oxidation to form a thin surface layer of silicon dioxide. These electrodes were tested in a rectangular flow cell under laminar flow conditions. The experimental steady-state response of these electrodes was evaluated by using flow injection methodology and compared with theoretical behavior predicted by backward implicit finite difference simulations. Currents and their dependence on flow rate show good agreement with theory. Aging tests of the electrodes indicate that the response decreased over a period of a few hours, but the electrodes remained active and showed no physical degradation after 24 h of continuous use.

Microelectrode arrays have received a great deal of attention as sensors for amperometric flow detectors in liquid chromatography and flow injection analysis (*1–10*). The theoretical response of microelectrode arrays in flow cells has been treated by a number of workers (*1, 2, 11–14*). The theory has been developed to characterize microelectrode arrays that have regularly spaced and sized active elements in the flow stream, for two fundamental geometries. The first geometry consists of a series of identical rectangular electrode elements maintained at a common applied potential and separated by rectangular gaps or electrochemically inactive sites (*1*). The second geometry consists of rectangular active elements separated by narrow gaps, where alternating elements are maintained at different potentials, also referred to as an interdigitated microelectrode array (*11*). Related work with rectangular strip electrodes has treated a single pair of electrodes in series at different potentials in a flow stream (*12*), an array of rectangular electrodes in a thin-layer cell in the absence of flow (*15*), an array in static solution (*16*), and polymer-coated arrays (*17–19*).

The microelectrode array flow sensors reported in the literature have included irregular arrays based on graphite powder (*4–7, 9, 10*), reticulated vitreous carbon (*3*), orderly

0003-2700/86/0358-2750$01.50/0